3

KINEMATICS

3.0 HISTORICAL DEVELOPMENT AND COMPLEXITY OF PROBLEM

Interest in the actual patterns of movement of humans and animals goes back to prehistoric times and was depicted in cave drawings, statues, and paintings. Such replications were subjective impressions of the artist. It was not until a century ago that the first motion picture cameras recorded locomotion patterns of both humans and animals. Marey, the French physiologist, used a photographic "gun" in 1885 to record displacements in human gait and chronophotographic equipment to get a stick diagram of a runner. About the same time, Muybridge in the United States triggered 24 cameras sequentially to record the patterns of a running man. Progress has been rapid during this century, and we now can record and analyze everything from the gait of a child with cerebral palsy to the performance of an elite athlete.

The term used for these descriptions of human movement is *kinematics.* Kinematics is not concerned with the forces, either internal or external, that cause the movement but rather with the details of the movement itself. A complete and accurate quantitative description of the simplest movement requires a huge volume of data and a large number of calculations, resulting in an enormous number of graphic plots. For example, to describe the movement of the lower limb in the sagittal plane during one stride can require up to 50 variables. These include linear and angular displacements, velocities, and accelerations. It should be understood that any given analysis may use only a

Biomechanics and Motor Control of Human Movement, Fourth Edition David A. Winter

Copyright © 2009 John Wiley & Sons, Inc. ISBN: 978-0-470-39818-0

small fraction of the available kinematic variables. An assessment of a running broad jump, for example, may require only the velocity and height of the body's center of mass. On the other hand, a mechanical power analysis of an amputee's gait may require almost all the kinematic variables that are available.

3.1 KINEMATIC CONVENTIONS

In order to keep track of all the kinematic variables, it is important to establish a convention system. In the anatomical literature, a definite convention has been established, and we can completely describe a movement using terms such as *proximal, flexion*, and *anterior.* It should be noted that these terms are all relative, that is, they describe the position of one limb relative to another. They do not give us any idea as to where we are in space. Thus, if we wish to analyze movement relative to the ground or the direction of gravity, we must establish an absolute spatial reference system. Such conventions are mandatory when imaging devices are used to record the movement. However, when instruments are attached to the body, the data become relative, and we lose information about gravity and the direction of movement.

3.1.1 Absolute Spatial Reference System

Several spatial reference systems have been proposed. The one utilized throughout the text is the one often used for human gait. The vertical direction is Y, the direction of progression (anterior–posterior) is X, and the sideways direction (medial–lateral) is Z. Figure 3.1 depicts this convention. The positive direction is as shown. Angles must also have a zero reference and a positive direction. Angles in the XY plane are measured from 0° in the X direction, with positive angles being counterclockwise. Similarly, in the YZ plane, angles start at 0° in the Y direction and increase positively counterclockwise. The convention for velocities and accelerations follows correctly if we maintain the spatial coordinate convention:

$\dot{x}$ = velocity in the X direction, positive when X is increasing
$\dot{y}$ = velocity in the Y direction, positive when Y is increasing
$\dot{z}$ = velocity in the Z direction, positive when Z is increasing
$\ddot{x}$ = acceleration in the X direction, positive when $\dot{x}$ is increasing
$\ddot{y}$ = acceleration in the Y direction, positive when $\dot{y}$ is increasing
$\ddot{z}$ = acceleration in the Z direction, positive when $\dot{z}$ is increasing

The same applies to angular velocities and angular accelerations. A counterclockwise angular increase is a positive angular velocity, $\boldsymbol{\omega}$. When $\boldsymbol{\omega}$ is increasing, we calculate a positive angular acceleration, $\boldsymbol{\alpha}$.

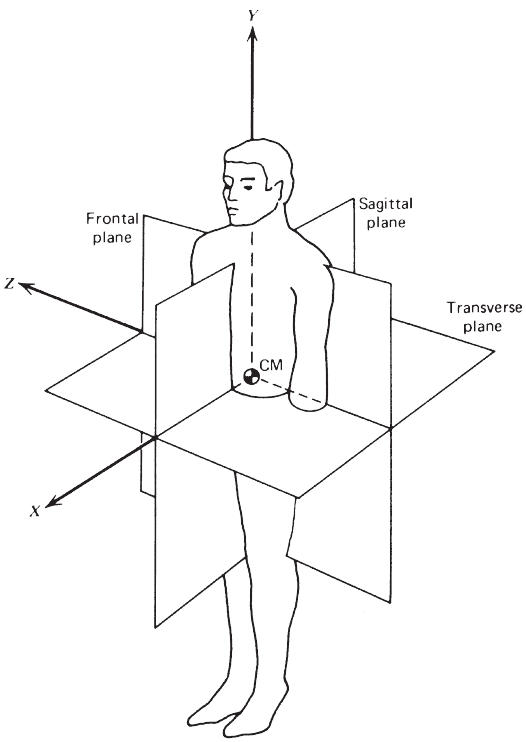

Figure 3.1 Spatial coordinate system for all data and analyses.

An example taken from the data on a human subject during walking will illustrate the convention. The kinematics of the right leg segment (as viewed from the right side) and its center of mass were analyzed as follows:

$$\boldsymbol{\omega} = -2.34 \text{ rad/s}, \quad \boldsymbol{\alpha} = 14.29 \text{ rad/s}^2, \quad \boldsymbol{v}_x = 0.783 \text{ m/s}$$
$$a_x = -9.27 \text{ m/s}^2, \quad \boldsymbol{v}_y = 0.021 \text{ m/s}, \quad a_y = -0.31 \text{ m/s}^2$$

This means that the leg segment is rotating clockwise but is decelerating (accelerating in a counterclockwise direction). The velocity of the leg's center of mass is forward and very slightly upward, but it is decelerating in the forward direction and accelerating downward.

3.1.2 Total Description of a Body Segment in Space

The complete kinematics of any body segment requires 15 data variables, all of which are changing with time:

1. Position (x, y, z) of segment center of mass
2. Linear velocity $(\dot{x}, \dot{y}, \dot{z})$ of segment center of mass

3. Linear acceleration $(\ddot{x}, \ddot{y}, \ddot{z})$ of segment center of mass
4. Angle of segment in two planes, $\boldsymbol{\theta}_{xy}, \boldsymbol{\theta}_{yz}$
5. Angular velocity of segment in two planes, $\boldsymbol{\omega}_{xy}, \boldsymbol{\omega}_{yz}$
6. Angular acceleration of segment in two planes, $\boldsymbol{\alpha}_{xy}, \boldsymbol{\alpha}_{yz}$

Note that the third angle data are redundant; any segment's direction can be completely described in two planes. For a complete description of the total body (feet + legs + thighs + trunk + head + upper arms + forearms and hands = 12 segments), movement in three-dimensional (3D) space required $15 \times 12 = 180$ data variables. It is no small wonder that we have yet to describe, let alone analyze, some of the more complex movements. Certain simplifications can certainly reduce the number of variables to a manageable number. In symmetrical level walking, for example, we can assume sagittal plane movement and can normally ignore the arm movement. The head, arms, and trunk (HAT) are often considered to be a single segment, and assuming symmetry, we need to collect data from one lower limb only. The data variables in this case (four segments, one plane) can be reduced to a more manageable 36.

3.2 DIRECT MEASUREMENT TECHNIQUES

3.2.1 Goniometers*

A goniometer is a special name given to the electrical potentiometer that can be attached to measure a joint angle. One arm of the goniometer is attached to one limb segment, the other to the adjacent limb segment, and the axis of the goniometer is aligned to the joint axis. In Figure 3.2, you can see the fitting of the goniometer to a knee joint along with the equivalent electrical circuit. A constant voltage E is applied across the outside terminals, and the wiper arm moves to pick off a fraction of the total voltage. The fraction of the voltage depends on the joint angle $\boldsymbol{\theta}$. Thus, the voltage on the wiper arm is $v = kE\boldsymbol{\theta} = k_1\boldsymbol{\theta}$ volts. Note that a voltage proportional to $\boldsymbol{\theta}$ requires a potentiometer whose resistance varies linearly with $\boldsymbol{\theta}$. A goniometer designed for clinical studies is shown fitted on a patient in Figure 3.3.

Advantages

1. A goniometer is generally inexpensive.
2. The output signal is available immediately for recording or conversion into a computer.
3. Planar rotation is recorded independently of the plane of movement of the joint.

*Representative paper: Finley and Karpovich, 1964.

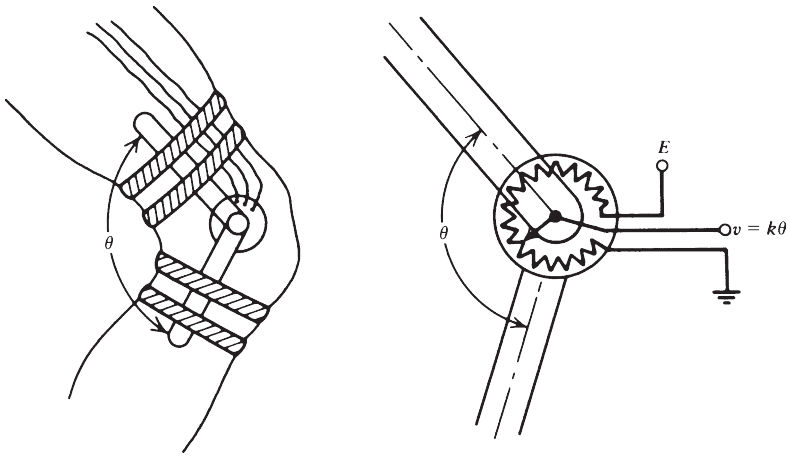

Figure 3.2 Mechanical and electrical arrangement of a goniometer located at the knee joint. Voltage output is proportional to the joint angle.

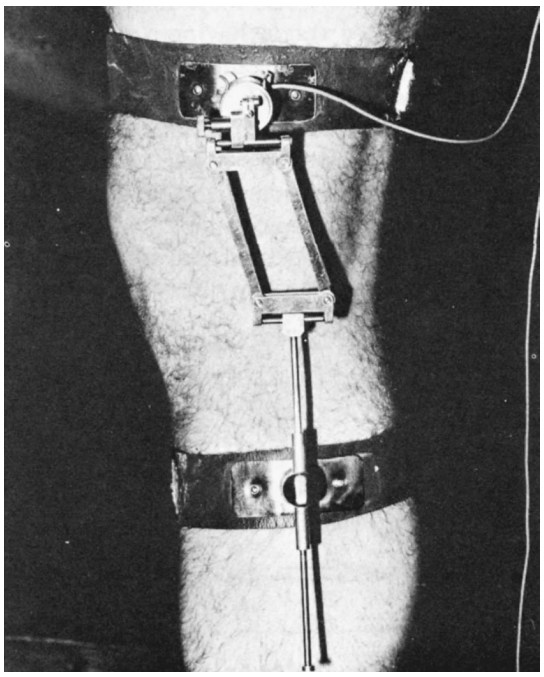

Figure 3.3 Electrogoniometer designed to accommodate changes in the axis of rotation of the knee joint, shown here fitted on a patient. (Reproduced by permission of Chedoke-McMaster Medical Center, Hamilton, Ont. Canada.)

Disadvantages

1. Relative angular data are given, not absolute angles, thus severely limiting the data's assessment value.
2. It may require an excessive length of time to fit and align, and the alignment over fat and muscle tissue can vary over the time of the movement.
3. If a large number are fitted, movement can be encumbered by the straps and cables.
4. More complex goniometers are required for joints that do not move as hinge joints.

3.2.2 Special Joint Angle Measuring Systems

More recently in the area of ergonomics, a special glove system has been developed to measure the kinematics of the fingers and the thumb. Figure 3.4 shows the construction of the glove transducer, which comprises a lightweight elastic glove with sensors on the proximal two joints of each finger and thumb plus a thumb abductor sensor. Each transducer is a loop of fiber-optic cable with a constant infrared source and is etched in the region of the joint of interest. As the joint flexes, the fiber bends and light escapes; the greater the bend, the more light that escapes. Thus, the flexion angular displacement is detected as a reduction in light intensity received by the detector and is precalibrated against the bending angle. A major use for such a system has been in the study of repetitive strain injuries (cf. Moore et al., 1991).

3.2.3 Accelerometers*

As indicated by its name, an accelerometer is a device that measures acceleration. Most accelerometers are nothing more than force transducers designed to measure the reaction forces associated with a given acceleration. If the acceleration of a limb segment is a and the mass inside is m, then the force exerted by the mass is $F = ma$. This force is measured by a force transducer, usually a strain gauge or piezoresistive type. The mass is accelerated against a force transducer that produces a signal voltage V, which is proportional to the force, and since m is known and constant, V is also proportional to the acceleration. The acceleration can be toward or away from the face of the transducer; the latter is indicated by a reversal in sign of the signal. In most movements, there is no guarantee that the acceleration vector will act at right angles to the face of the force transducer. The more likely situation is depicted in Figure 3.5, with the acceleration vector having a component normal to the transducer and another component tangent to the transducer face. Thus, the accelerometer measures the a_n component. Nothing is known

*Representative paper: Morris, 1973.

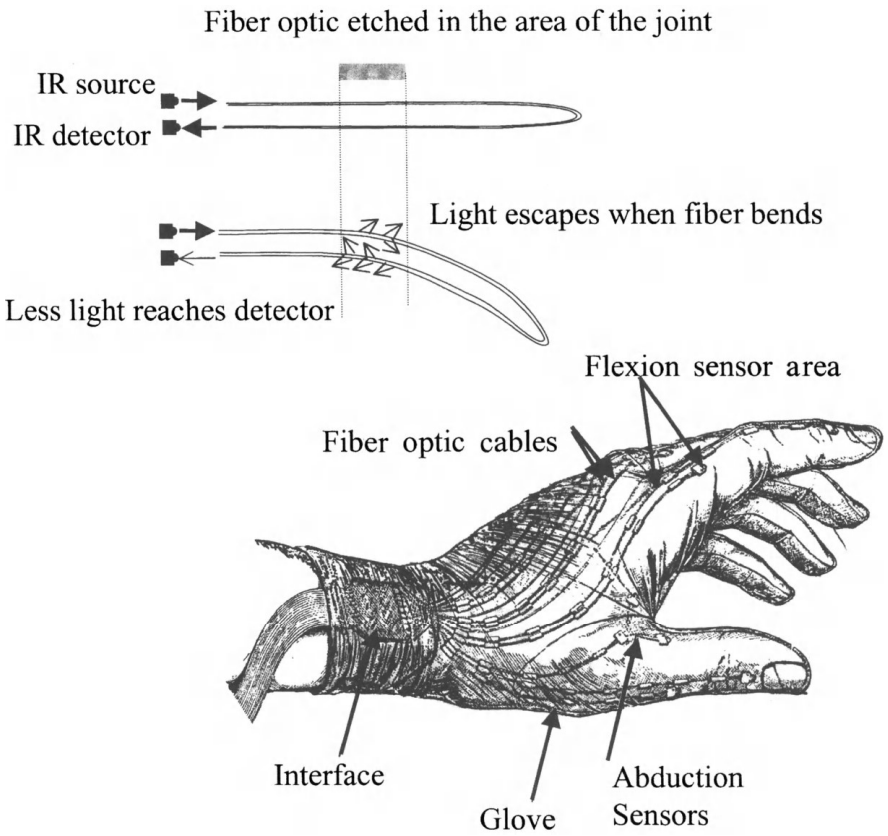

Figure 3.4 Construction and operation of a glove transducer to measure angular displacements of the fingers. Transducer is a loop of fiber-optic cable; the amount of light returning to the detector decreases with increased finger flexion. Each cable is calibrated for angular displacement versus detected light intensity. (Courtesy of the Ergonomics Laboratory, Department of Kinesiology, University of Waterloo, Waterloo, Ont. Canada.)

about a_t or a unless a triaxial accelerometer is used. Such a 3D transducer is nothing more than three individual accelerometers mounted at right angles to each other, each one then reacting to the orthogonal component acting along its axis. Even with a triaxial accelerometer mounted on a limb, there can be problems because of limb rotation, as indicated in Figure 3.6. In both cases, the leg is accelerating in the same *absolute* direction, as indicated by vector a. The measured acceleration component a_n is quite different in each case. Thus, the accelerometer is limited to those movements whose direction in space does not change drastically or to special contrived movements, such as horizontal flexion of the forearm about a fixed elbow joint.

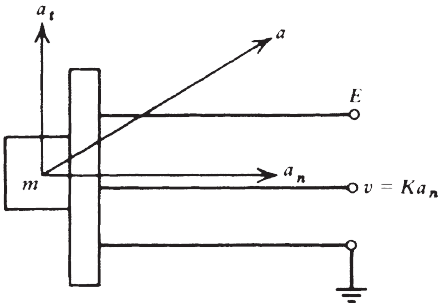

Figure 3.5 Schematic diagram of an accelerometer showing acceleration with normal and tangential components. Voltage output is proportional to the normal component of acceleration, a_n.

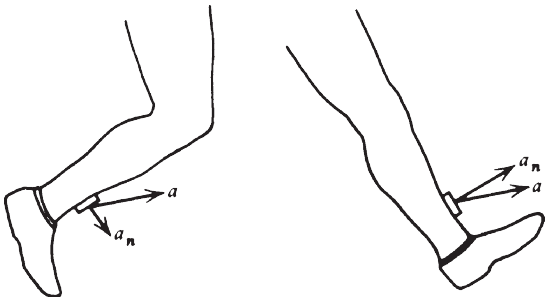

Figure 3.6 Two movement situations where the acceleration in space is identical but the normal components are quite different.

A typical electric circuit of a piezoresistive accelerometer is shown in Figure 3.7. It comprises a half-bridge consisting of two equal resistors R_1. Within the transducer, resistors R_a and R_b change their resistances proportionally to the acceleration acting against them. With no acceleration, $R_a = R_b = R_1$, and with the balance potentiometer properly adjusted, the voltage at terminal 1 is the same as that at terminal 2. Thus, the output voltage is $V = 0$. With the acceleration in the direction shown, R_b increases and R_a decreases; thus, the voltage at terminal 1 increases. The resultant imbalance in the bridge circuit results in voltage V, proportional to the acceleration. Conversely, if the acceleration is upward, R_b decreases and R_a increases; the bridge unbalances in the reverse direction, giving a signal of the opposite polarity. Thus, over the dynamic range of the accelerometer, the signal is proportional to both the magnitude and the direction of acceleration acting along the axis of the accelerometer. However, if the balance potentiometer is not properly set, we have an unbalanced bridge and we could get a voltage-acceleration relationship like that indicated by the dashed lines.

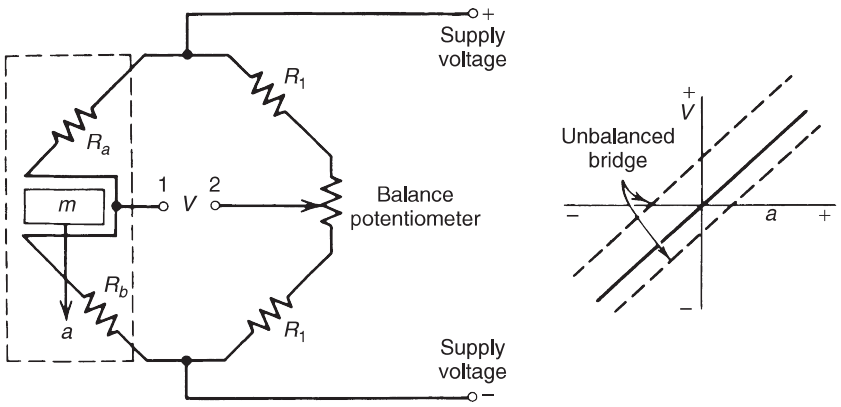

Figure 3.7 Electrical bridge circuit used in most force transducers and accelerometers. See text for detailed operation.

Advantages

1. Output signal is available immediately for recording or conversion into a computer.

Disadvantages

1. Acceleration is relative to its position on the limb segment.
2. Cost of accelerometers can be excessive if a large number are used; also the cost of the recorder or analog-to-digital converter may be high.
3. If a large number are used, they can encumber movement.
4. Many types of accelerometers are quite sensitive to shock and are easily broken.
5. The mass of the accelerometer may result in a movement artifact, especially in rapid movements or movements involving impacts.

3.3 IMAGING MEASUREMENT TECHNIQUES

The Chinese proverb "A picture is worth more than ten thousand words" holds an important message for any human observer, including the biomechanics researcher interested in human movement. Because of the complexity of most movements, the only system that can possibly capture all the data is an imaging system. Given the additional task of describing a dynamic activity, we are further challenged by having to capture data over an extended period of time. This necessitates taking many images at regular intervals during the event.

There are many types of imaging systems that could be used. The discussion will be limited to three different types: movie camera, television, and

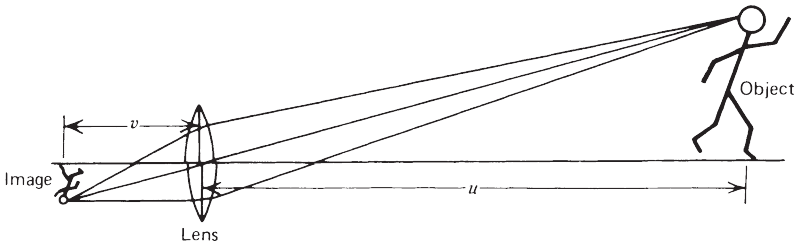

Figure 3.8 Simple focusing lens system showing relationship between the object and image.

optoelectric types. Whichever system is chosen, a lens is involved; therefore, a short review of basic optics is given here.

3.3.1 Review of Basic Lens Optics

A simple converging lens is one that creates an inverted image in focus at a distance v from the lens. As seen in Figure 3.8, if the lens—object distance is u, then the focal length f of the lens is:

$$\frac{1}{f} = \frac{1}{v} + \frac{1}{u} \tag{3.1}$$

The imaging systems used for movement studies are such that the object—lens distance is quite large compared with the lens—image distance. Therefore,

$$\frac{1}{u} \approx 0, \quad \frac{1}{f} = \frac{1}{v}, \quad \text{or } f = v \tag{3.2}$$

Thus, if we know the focal length of the lens system, we can see that the image size is related to the object size by a simple triangulation. A typical focal length is 25 mm, a wide-angle lens is 13 mm, and a telephoto lens is 150 mm. A zoom lens is just one in which the focal length is infinitely variable over a given range. Thus, as L increases, the focal length must increase proportionately to produce the same image size. Figure 3.9 illustrates this principle. For maximum accuracy, it is highly desirable that the image be as large as possible. Thus, it is advantageous to have a zoom lens rather than a series of fixed lenses; individual adjustments can be readily made for each movement to be studied, or even during the course of the event.

3.3.2 f-Stop Setting and Field of Focus

The amount of light entering the lens is controlled by the lens opening, which is measured by its f-stop (f means fraction of lens aperture opening).

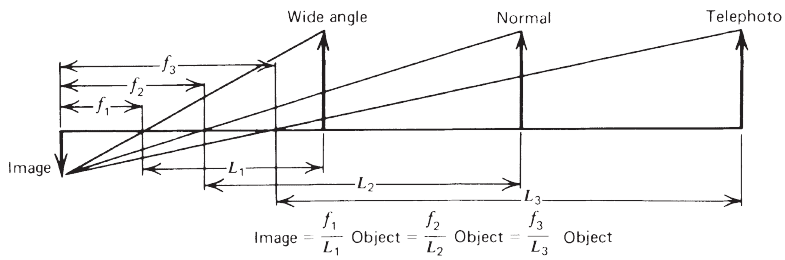

Figure 3.9 Differences in the focal length of wide angle, normal, and telephoto lenses result in an image of the same size.

The larger the opening, the lower the f-stop setting. Each f-stop setting corresponds to a proportional change in the amount of light allowed in. A lens may have the following settings: 22, 16, 11, 8, 5.6, 4, 2.8, and 2. $f/22$ is 1/22 of the lens diameter, and $f/11$ is 1/11 of the lens diameter. Thus $f/11$ lets in four times the light that $f/22$ does. The fractions are arranged so that each one lets in twice the light of the adjacent higher setting (e.g., $f/2.8$ provides twice the light of $f/4$).

To keep the lighting requirements to a minimum, it is obvious that the lens should be opened as wide as possible with a low f setting. However, problems occur with the field of focus. This is defined as the maximum and minimum range of the object that will produce a focused image. The lower the f setting, the narrower the range over which an object will be in focus. For example, if we wish to photograph a movement that is to move over a range from 10 to 30 ft, we cannot reduce the f-stop below 5.6. The range set on the lens would be about 15 ft, and everything between 10 and 30 ft would remain in focus. The final decision regarding f-stop depends on the shutter speed of the movie camera and the film speed.

3.3.3 Cinematography*

Many different sizes of movie cameras are available; 8-mm cameras are the smallest. (They actually use 16-mm film, which is run through the camera twice, then split into two 8-mm strips after it is developed.) Then there are 16 mm, 35 mm, and 70 mm. The image size of 8 mm is somewhat small for accurate measurements, while 35-mm and 70-mm movie cameras are too expensive to buy and operate. Thus, 16-mm cameras have evolved as a reasonable compromise, and most high-speed movie cameras are 16 mm. There are several types of 16-mm cameras available. Some are spring driven; others are motor driven by either batteries or power supplies from alternating current sources. Battery-driven types have the advantage of being portable to sites where power is not available.

*Representative paper: Eberhart and Inman, 1951.

The type of film required depends on the lighting available. The ASA rating is a measure of the *speed* of the film; the higher the rating, the less light is required to get the same exposure. 4-X reversal film with an ASA rating of 400 is a common type. Higher ASA ratings are also available and are good for a qualitative assessment of movement, especially faster-moving sporting events. However, the coarse grain of these higher ASA films introduces inaccuracies in quantitative analyses.

The final factor that influences the lighting required is the shutter speed of the camera. The higher the frame rate, the less time that is available to expose film. Most high-speed cameras have rotating shutters that open once per revolution for a period of time to expose a new frame of unexposed film. The arc of the opening, as depicted in Figure 3.10, and the speed of rotation of the shutter decide the exposure time. For example, at 60 frames per second, using a 3 factor shutter, the exposure time is 1/180 s. The amount of light entering will be the same as a normal (still) camera set to a speed of 1/180 s.

To make the final settings, we use an exposure meter to measure the light intensity on the human subject. For a given filming, the variables that are preset are film ASA, shutter factor, and frame rate. The frame rate is set low enough to capture the desired event but not so high as to require extra lighting or result in film wastage. To understand the problem associated with the selection of an optimal rate, the student is referred back to Section 2.2.4.2 on the sampling theorem. The final variable to decide is the f-stop. The light meter gives an electrical meter reading proportional to the light intensity, such that when the film ASA and exposure time are set, the correct f-stop

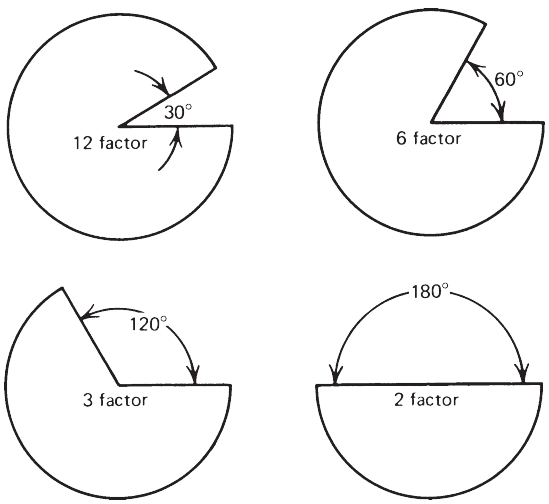

Figure 3.10 Various-factor shutters used in movie cameras. Film is exposed during the opening arc and is advanced while the shutter in closed.

can be determined. Thus, with the movie camera set at the right frame rate, f-stop, and range, the filming is ready to commence.

3.3.3.1 Movie Conversion Techniques. As 16-mm movie cameras are the most common form of data collection, it is important to be aware of various coordinate extraction techniques. Each system that has evolved requires the projection of each movie frame on some form of screen. The most common type requires the operator to move a mechanical xy coordinate system until a point, a light, or cross hairs lies over the desired anatomical landmark. Then the x and y coordinates can be read off or transferred to a computer at the push of a button. Figure 3.11 shows the component parts of such a conversion system.

A second type of system involves the projection of the film image onto a special grid system. When the operator touches the grid with a special pen, the coordinates are automatically transferred into a computer. Both systems are limited to the speed and accuracy of the human operator. Our experience indicates that an experienced operator can convert an average of 15 coordinate pairs per minute. Thus a 3-s film record filmed at 50 frames per second could have five markers converted in 30 min.

Figure 3.11 Typical arrangement for the microcomputer digitization of data coordinates from movie film. Foot pedal allows operator to transfer coordinate data to the computer at a rate of about 10 coordinate pairs per minute. Digitizing error is about 1 mm rms with the camera located 4 m from the subject.

The human error involved in this digitizing has been found to be random and quite small. For a camera 4 m from a subject, the root-mean-square (rms) "noise" present in the converted data has been measured at 1–1.5 mm.

3.3.4 Television*

The major difference between television and cinematography is the fact that television has a fixed frame rate. The name given to each television image is a field. In North America, there are 60 fields per second; in Europe, the standard is 50 fields per second. Thus, television has a high enough field rate for most movements, but it is probably too low for a quantitative analysis of rapid athletic events. The f-stop, focus, and lighting for television can be adjusted by watching the television monitor as the controls are varied. Many television cameras have electronic as well as optical controls that influence brightness and contrast, and some have built-in strobe lighting. Also, focus can be adjusted electronically as well as optically. The major advantage of television is the capability for instant replay, which serves both as a quality control check and as an initial qualitative assessment. Second, the television signal can be digitally converted by a "frame grabber" for immediate analysis.

3.3.4.1 Television Imaging Cameras. Some technical problems can result from the use of standard vidicon television cameras. The strong signal from a reflective marker produces a distinct circular image when the marker is not moving. However, when there is a rapid marker movement, the circular image blurs and produces a trailing edge. Thus, the triggering threshold for conversion into two levels (black and white) must be carefully set to ensure a circular digitized image. A more reliable way to get rid of the blur is to use a strobe system, which results in the exposure of the TV imaging tube for a millisecond or less. The strobe, in effect, acts as an electronic shutter. Strobe systems also eliminate a second problem associated with a continuously exposed imaging tube: skewing of the marker coordinates because of the time delay in the scanning from the top of the image to the bottom of the image. It takes about 15 ms to scan one TV field; thus, a head marker could be scanned 10 ms before a foot marker. The strobe system freezes all marker images at the same point in time in the same way that a movie camera does. Newer charge coupled diode (CCD) cameras have mechanical or electronic shutter controls that eliminate both blurring and skewing. A further development is the infrared camera, which does not use visible light and is not influenced by reflections from light sources other than those sources required to get the desired circular reflection from the markers. Figure 3.12 shows a typical infrared camera mounted permanently from the ceiling in a clinical gait laboratory. The active infrared lights form a "donut" shape about the camera lens and are pulsed at 120 Hz for a period of less than a millisecond.

*Representative paper: Winter et al., 1972.

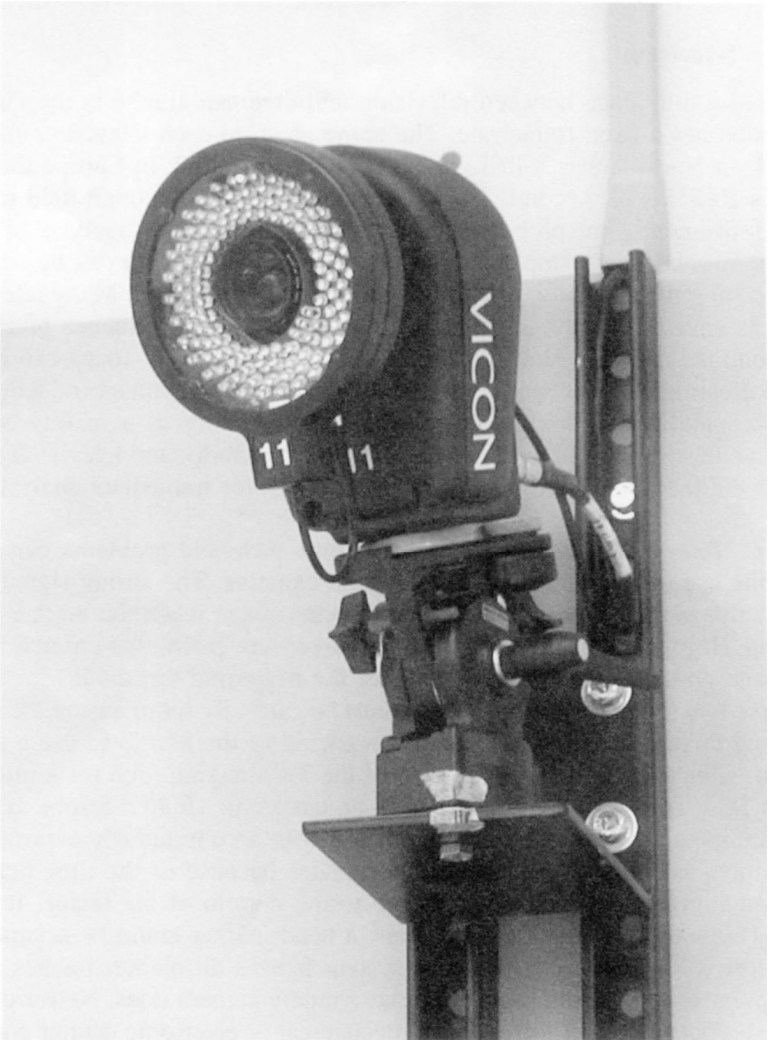

Figure 3.12 Typical infrared television camera mounted permanently in a clinical gait laboratory. The infrared lights form a "donut" shape around the lens and are pulsed for a short time each frame to freeze the image prior to scanning. (Courtesy of the Gait Analysis Laboratory, Connecticut Children's Medical Center, Hartford, CT.)

This camera is one of six to twelve cameras that could be mounted around the gait laboratory. Thus, the reflected infrared light from the markers is the only light that is picked up by the camera, and since it is a pulsed source, the marker images are "frozen" in time. Figure 3.13 depicts such an arrangement in a clinical gait laboratory along with the spherical reflective markers mounted on a young patient.

Figure 3.13 Gait assessment of a cerebral palsy patient in a clinical gait laboratory. Infrared cameras on the ceiling and walls capture the reflected light from the spherical reflective markers mounted on both sides of the body. (Courtesy of the Gait Analysis Laboratory, Connecticut Children's Medical Center, Hartford, CT.)

3.3.4.2 Historical Development of Television Digitizing Systems. Almost all of the movement analysis television systems were developed in university research laboratories. In the late 1960s, the first reports of television-based systems started to appear: at Delft University of Technology in The Netherlands (Furnée, 1967, according to Woltring, 1987) and at the Twenty-First Conference EMB in Houston, Texas (Winter et al., 1968). The first published paper on an operational system was by Dinn et al. (1970) from the Technical University of Nova Scotia in Halifax, Nova Scotia, Canada. It was called CINTEL (Computer INterface for TELivision) and was developed for digitizing angiographic images at 4 bits (16 grey levels) to determine the time course of left ventricular volume (Trenholm et al., 1972). It was also used for

gait studies at the University of Manitoba in Winnipeg, Manitoba, Canada, where, with higher spatial resolution and a one-bit (black/white) conversion, the circular image of a reflective hemispheric ping pong ball attached on anatomical landmarks was digitized (Winter et al., 1972). With about 10 pixels within each marker image, it was possible by averaging their coordinates to improve the spatial precision of each marker from 1 cm (distance between scan lines of each field) to about 1 mm. The 3M Scotch® material that was used as reflective material has been used by most subsequent experimental and commercial systems.

Jarett et al. (1976) reported a system that detected the left edge of the image of a small reflective marker that occupied one or two scan lines. Unfortunately, the spatial precision was equal to the scan line distance, which is about 1 cm. This system was adopted and improved by VICON (VIdeo CONvertor) in their commercial system. Both left and right edges of the marker image were detected, and subsequently the detected points were curve fitted via software AMASS to a circle (Macleod et al., 1990). Based on the circle fit, the centroid was calculated. Other commercial systems, such as the one developed by the Motion Analysis Corporation, use patented edge-detection techniques (Expert Vision). Shape recognition of the entire marker image, rather than edge detection, was used by the ELITE (Elaboratore di Immagini Televisive) system developed in Milan, Italy. A dedicated computer algorithm operating in real time used a cross-correlation pattern recognition technique based on size and shape (Ferrigno and Pedotti, 1985). This system uses all grey levels in the shape detection, thus improving the spatial resolution to 1/2800 of the viewing field. If we consider the field height to be about 2.5 m, this represents a precision of about 0.9 mm.

3.3.4.3 Television Conversion Techniques. Each of the commercial television systems that were mentioned in the previous section has it own unique technique for identifying the presence of a marker and determining its centroid, and for labeling markers from a multi-camera system.

3.3.5 Optoelectric Techniques*

In the past few years, there have been several developments in optoelectric imaging systems that have some advantages over cinematography and television. The first commercial system was developed by Northern Digital in Waterloo, Ontario, Canada, and was called Watsmart. It was an active system that required the subject to wear tiny infrared lights on each desired anatomical landmark. The lights were flashed sequentially, and the light flash was detected on a special camera. The camera consisted of a standard lens focusing the light flash onto a special semiconductor diode surface. More recent development of this active system has resulted in a 3D camera system

*Representative paper: Winter et al., 2003.

called OPTOTRAK. Such a system consists of three cameras mounted in line on a rigid frame, as shown in Figure 3.14. The left and right lenses are mounted to face slightly inward and their linear diode arrays are mounted horizontally. Thus, their scan of the pulsed light will define the location of a marker in a vertical plane. The middle lens is mounted with its diode array mounted vertically, and its scan will define a horizontal plane. Figure 3.15 depicts this arrangement. The left and right detectors each define the location of all markers in a vertical plane; the intersection of these two vertical planes is a vertical line. Thus, any markers on this vertical line will record the same signal on the left and right cameras. The middle camera has its lens facing directly ahead with its diode array mounted vertically. Thus, this camera will define all markers in a horizontal plane. The intersection of this horizontal plane with the vertical line defined by the other two cameras is a unique 3D point in space. Thus, as each infrared diode (IRED) pulses, its x, y, z coordinates in the global reference system (GRS) are recorded. The pulsed light from a second light source yields a different vertical line and horizontal plane and, thus, a different set of x, y, z coordinates. There are some unique advantages to such an active system. There is no specialized software required (as in television) to identify which marker is which. Thus, in laboratories where

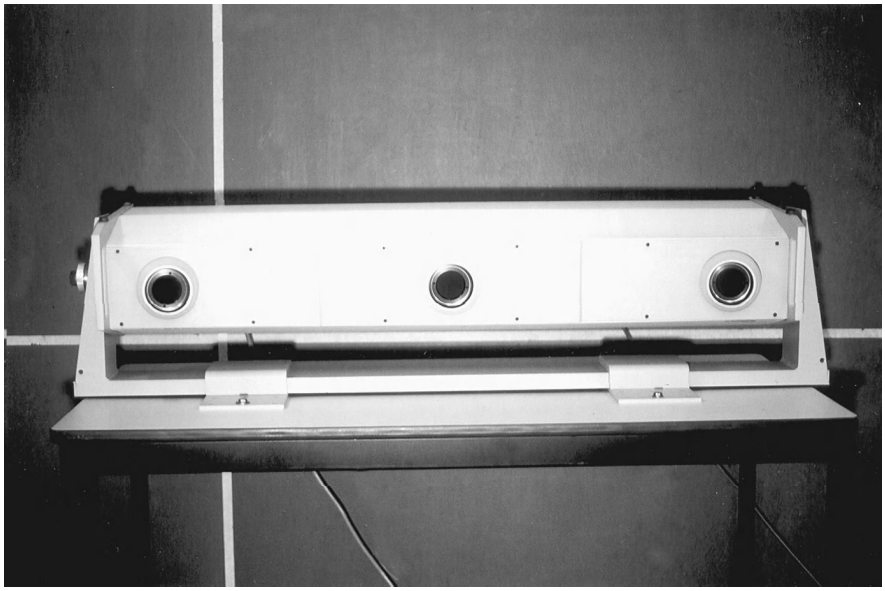

Figure 3.14 An OPTOTRAK system with three lenses, each with a linear diode array. The outside two lenses face slightly inward and each defines a vertical plane, while the middle lens defines a horizontal plane. See Figure 3.15 to see how these three diode arrays define a marker in 3D space. (Courtesy of the Gait and Posture Laboratory, Department of Kinesiology, University of Waterloo, Waterloo, Ont., Canada.)

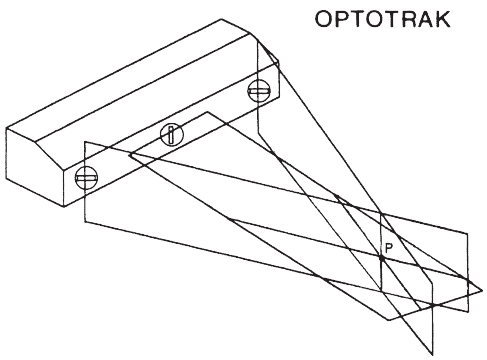

Figure 3.15 OPTOTRAK system with two outside lenses facing slightly inward with their diode arrays, each defining markers in a vertical plane. Any marker on the intersection of these two planes will define all markers on this vertical line. The middle lens array defines all markers in a horizontal plane. Thus, the intersection of a marker on this horizontal plane with the vertical line will define the unique coordinates of a marker in 3D space.

the number and location of markers is changing from day to day, there are no problems with marker labeling, which makes this system flexible for the changing research requirements. Also, because of the precision of the IRED array, the precision of the x, y, z coordinates is better than that of TV systems, which are constrained by the distance between the scan lines. The precision for an OPTOTRAK camera mounted as shown in Figure 3.15 at a distance of 4 m from the subject is 0.03 mm with noise = 0.015 mm (Gage et al., 2004). Possible disadvantages are the number of IREDs that can be mounted and the potential encumbrance of the cables connecting the power source to the active IREDs.

3.3.6 Advantages and Disadvantages of Optical Systems

Advantages

1. All data are presented in an absolute spatial reference system, in a plane normal to the optical axis of the camera.
2. Most systems (cine, TV) are not limited as to the number of markers used.
3. Encumbrance to movement is minimal for most systems that use lightweight reflective markers (cine, TV), and the time to apply the markers is minimal.
4. TV cameras and VCRs are reasonably inexpensive.
5. Cine and TV systems can be replayed for teaching purposes or for qualitative analysis of the total body movement.

Disadvantages

1. Most multiple-camera systems are expensive (cine, TV, optoelectric), as are the digitizing and conversion systems for all imaging sources.
2. For film, the turnaround time for development may be a problem, and the labor to digitize film coordinates may also be a constraint. The digitizing errors, however, are less than those from many commercial imaging systems.
3. Encumbrance and time to fit wired light sources (e.g., IREDs) can be prohibitive in certain movements, and the number of light sources is limited.
4. Some imaging systems (e.g., IREDs) cannot be used outside in daylight.

3.3.7 Summary of Various Kinematic Systems

Each laboratory must define its special requirements before choosing a particular system. A clinical gait lab may settle on TV because of the encumbrance of optoelectric systems and because of the need for a qualitative assessment, rapid turnaround, and teaching. Ergonomic and athletic environments may require instant or near-instant feedback to the subject or athlete, thus dictating the need for an automated system. Basic researchers do not require a rapid turnaround and may need a large number of coordinates; thus, they may opt for movie cameras or an optoelectric system. And, finally, the cost of hardware and software may be the single limiting factor that may force a compromise as to the final decision.

3.4 PROCESSING OF RAW KINEMATIC DATA

3.4.1 Nature of Unprocessed Image Data

Film and television are sampling processes. They capture the movement event for a short period of time, after which no further changes are recorded until the next field or frame. Playing a movie film back slowly demonstrates this phenomenon: the image jumps from one position to the next in a distinct step rather than a continuous process. The only reason that film or television does not appear to jump at normal projection speeds (24 per second for film, 60 per second for television) is because the eye can retain an image for a period of about 1/15 s. The eye's short-term "memory" enables the human observer to average or smooth out the jumping movement.

The converted coordinate data from film or television are called *raw* data. This means that they contain additive noise from many sources: electronic noise in optoelectric devices, spatial precision of the TV scan or film digitizing system, or human error in film digitizing. All of these will result in random

errors in the converted data. It is, therefore, essential that the raw data be smoothed, and in order to understand the techniques used to smooth the data, an appreciation of harmonic (or frequency) analysis is necessary. The theory of harmonic analyses has been covered in Section 2.2; however, there are some additional special problems with the processing of kinematic data that are now discussed.

3.4.2 Signal versus Noise in Kinematic Data

In the study of movement, the signal may be an anatomical coordinate that changes with time. For example, in running, the Y (vertical) coordinate of the heel will have certain frequencies that will be higher than those associated with the vertical coordinate of the knee or trunk. Similarly, the frequency content of all trajectories will decrease in walking compared with running. In repetitive movements, the frequencies present will be multiples (harmonics) of the fundamental frequency (stride frequency). When walking at 120 steps per minute (2 Hz), the stride frequency is 1 Hz. Therefore, we can expect to find harmonics at 2 Hz, 3 Hz, 4 Hz, and so on. Normal walking has been analyzed by digital computer, and the harmonic content of the trajectories of seven leg and foot markers was determined (Winter et al., 1974). The highest harmonics were found to be in the toe and heel trajectories, and it was found that 99.7% of the signal power was contained in the lower seven harmonics (below 6 Hz). The harmonic analysis for the toe marker for 20 subjects is shown in Figure 3.16, which is the same as Figure 2.17 and is repeated to show the noise content. Above the seventh harmonic, there was still some signal power, but it had the characteristics of "noise." Noise is the term used to describe components of the final signal that are not due to the process

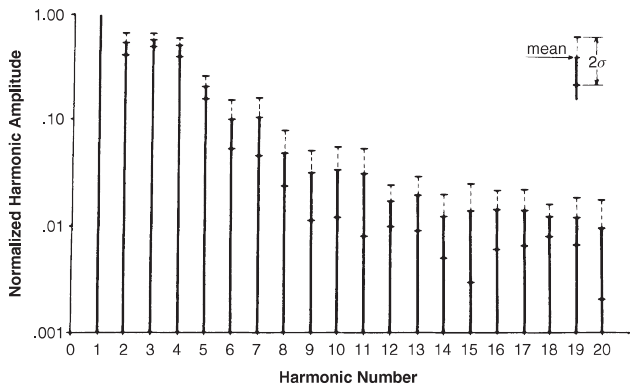

Figure 3.16 Harmonic content of the vertical displacement of a toe marker from 20 subjects during normal walking. Fundamental frequency (harmonic number = 1) is normalized at 1.00. Over 99% of the power is contained below the seventh harmonic. (Reproduced by permission from the *Journal of Biomechanics.*)

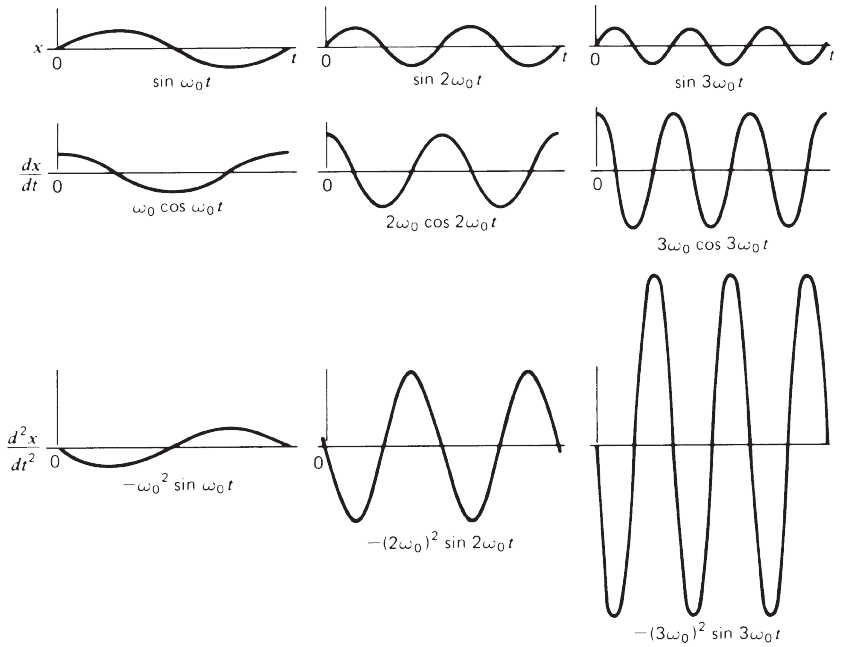

Figure 3.17 Relative amplitude changes as a result of the time differentiation of signals of increasing frequency. The first derivative increases the amplitude proportional to frequency; the second derivative increases the amplitude proportionally to frequency squared. Such a rapid increase has severe implications in calculating accelerations when the original displacement signal has high-frequency noise present.

itself (in this case, walking). Sources of noise were noted in Section 3.4.1, and if the total effect of all these errors is random, then the true signal will have an added random component. Usually the random component is high frequency, as is borne out in Figure 3.16. Here you can see evidence of higher-frequency components extending up to the 20th harmonic, which was the highest frequency analyzed.

3.4.3 Problems of Calculating Velocities and Accelerations

The presence of this higher-frequency noise is of considerable importance when we consider the problem of trying to calculate velocities and accelerations. Consider the process of time differentiation of a signal containing additive higher-frequency noise. Suppose that the signal can be represented by a summation of N harmonics:

$$x = \sum_{n=1}^{N} X_n \sin(n\omega_0 t + \theta_n) \tag{3.3}$$

where: $\boldsymbol{\omega}_o$ = fundamental frequency
n = harmonic number
X_n = amplitude of nth harmonic
$\boldsymbol{\theta}_n$ = phase of nth harmonic

To get the velocity in the x direction V_x, we differentiate with respect to time:

$$V_x = \frac{dx}{dt} = \sum_{n=1}^{N} n\boldsymbol{\omega}_0 X_n \cos(n\boldsymbol{\omega}_0 t + \boldsymbol{\theta}_n) \tag{3.4}$$

Similarly, the acceleration A_x is:

$$A_x \frac{dV_x}{dt} = -\sum_{n=1}^{N} (n\boldsymbol{\omega}_0)^2 X_n \sin\ (n\boldsymbol{\omega}_0 t + \boldsymbol{\theta}_n) \tag{3.5}$$

Thus, the amplitude of each of the harmonics increases with its harmonic number; for velocities they increase linearly, and for accelerations the increase is proportional to the square of the harmonic number. This phenomenon is demonstrated in Figure 3.17, where the fundamental, second, and third harmonics are shown, along with their first and second time derivatives. Assuming that the amplitude x of all three components is the same, we can see that the first derivative (velocity) of harmonics increases linearly with increasing frequency. The first derivative of the third harmonic is now three times that of the fundamental. For the second time derivative, the increase repeats itself, and the third harmonic acceleration is now nine times that of the fundamental.

In the trajectory data for gait, x_1 might be 5 cm and $x_{20} = 0.5$ mm. The 20th harmonic noise is hardly perceptible in the displacement plot. In the velocity calculation, the 20th harmonic increases 20-fold so that it is now one-fifth that of the fundamental. In the acceleration calculation, the 20th harmonic increases by another factor of 20 and now is four times the magnitude of the fundamental. This effect is shown if you look ahead to Figure 3.19, which plots the acceleration of the toe during walking. The random-looking signal is the raw data differentiated twice. The smooth signal is the acceleration calculated after most of the higher-frequency noise has been removed. Techniques to remove this higher-frequency noise are now discussed.

3.4.4 Smoothing and Curve Fitting of Data

The removal of noise can be accomplished in several ways. The aims of each technique are basically the same. However, the results differ somewhat.

3.4.4.1 Curve-Fitting Techniques. The basic assumption here is that the trajectory signal has a predetermined shape and that by fitting the assumed shape to a "best fit" with the raw noisy data, a smooth signal will result. For example, it may be assumed that the data are a certain order polynomial:

$$x(t) = a_0 + a_1 t + a_2 t^2 + a_3 t^3 + \cdots + a_n t^n \tag{3.6}$$

By using computer techniques, the coefficients $a_0, \ldots, a_n$ can be selected to give a best fit, using such criteria as minimum mean square error.

A second type of curve fit can be made assuming that a certain number of harmonics are present in the signal. Reconstituting the final signal as a sum of N lowest harmonics,

$$x(t) = a_0 + \sum_{n=1}^{N} a_n \sin\,(n\omega_0 t + \theta_n) \tag{3.7}$$

This model has a better basis, especially in repetitive movement, while the polynomial may be better in certain nonrepetitive movement such as broad jumping. However, there are severe assumptions regarding the consistency (stationarity) of a_n and θ_n, as was discussed previously in Section 2.2.4.5.

A third technique, spline curve fitting, is a modification of the polynomial technique. The curve to be fitted is broken into sections, each section starting and ending with an inflection point, with special fitting being done between adjacent sections. The major problem with this technique is the error introduced by improper selection of the inflection points. These inflection points must be determined from the noisy data and, thus, are strongly influenced by the very noise that we are trying to eliminate.

3.4.4.2 Digital Filtering—Refiltering to Remove Phase Lag of Low-Pass Filter. The fourth and most common technique used to attenuate the noise is digital filtering, which was introduced in Section 2.2.4.4. Digital filtering is not a curve-fitting technique like the three discussed above but is a noise attenuation technique based on differences in the frequency content of the signal versus the noise. However, there are some additional problems related to the low-pass filtering of the raw kinematic coordinates, and these are now discussed. For the sake of convenience the formulae necessary to calculate the five coefficients of a second-order filter are repeated here:

$$\omega_c = \frac{(\tan(\pi f_c / f_s))}{C} \tag{3.8}$$

where C is the correction factor for number of passes required, to be explained shortly. For a single-pass, filter $C = 1$.

$$K = \sqrt{2}\omega_c \text{ for a Butterworth filter}$$

$$\text{or, } 2\omega_c \text{ for a critically damped filter}$$

$$K_2 = \omega_c^2, \quad a_0 = \frac{K_2}{(1 + K_1 + K_2)}, \quad a_1 = 2a_0, \quad a_2 = a_0$$

$$K_3 = \frac{2a_0}{K_2}, \quad b_1 = -2a_0 + K_3$$

$$b_2 = 1 - 2a_0 - K_3, \quad \text{or} \quad b_2 = 1 - a_0 - a_1 - a_2 - b_1$$

As well as attenuating the signal, there is a phase shift of the output signal relative to the input. For this second-order filter there is a 90° phase lag at the cutoff frequency. This will cause a second form distortion, called *phase distortion*, to the higher harmonics within the bandpass region. Even more phase distortion will occur to those harmonics above f_c, but these components are mainly noise, and they are being severely attenuated. This phase distortion may be more serious than the amplitude distortion that occurs to the signal in the transition region. To cancel out this phase lag, the once-filtered data was filtered again, but this time in the reverse direction of time (Winter et al., 1974). This introduces an equal and opposite phase lead so that the net phase shift is zero. Also, the cutoff of the filter will be twice as sharp as that for single filtering. In effect, by this second filtering in the reverse direction, we have created a fourth-order zero-phase-shift filter, which yields a filtered signal that is back in phase with the raw data but with most of the noise removed.

In Figure 3.18 we see the frequency response of a second-order Butter-worth filter normalized with respect to the cutoff frequency. Superimposed on this curve is the response of the fourth-order zero-phase-shift filter. Thus, the new cutoff frequency is lower than that of the original single-pass filter; in this case, it is about 80% of the original. The correction factor for each additional pass of a Butterworth filter is $C = (2^{1/n} - 1)^{0.25}$, where n is the number of passes. Thus, for a dual pass, $C = 0.802$. For a critically damped filter, $C = (2^{1/2n} - 1)^{0.5}$; thus, for a dual pass, $C = 0.435$. This correction factor is applied to Equation (3.8) and results in the cutoff frequency for the original single-pass filter being set higher, so that after the second pass the desired cutoff frequency is achieved. The major difference between these two filters is a compromise in the response in the time domain. Butterworth filters have a slight overshoot in response to step- or impulse-type inputs, but they have a much shorter rise time. Critically damped filters have no overshoot but suffer from a slower rise time. Because impulsive-type inputs are rarely seen in human movement data, the Butterworth filter is preferred.

The application of one of these filters in smoothing raw coordinate data can now be seen by examining the data that yielded the harmonic plot in Figure 3.16. The horizontal acceleration of this toe marker, as calculated by

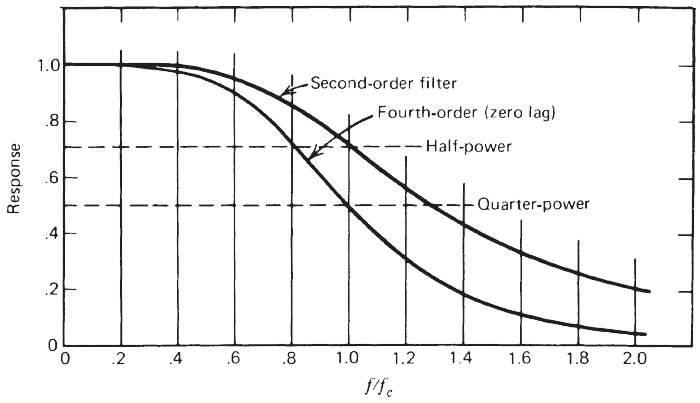

Figure 3.18 Response of a second-order low-pass digital filter. Curve is normalized at 1.0 at the cutoff frequency, *fc*. Because of the phase lag characteristics of the filter, a second refiltering is done in the reverse direction in time, which results in a fourth-order zero-lag filter.

finite differences from the filtered data, is plotted in Figure 3.19. Note how repetitive the filtered acceleration is and how it passes through the "middle" of the noisy curve, as calculated using the unfiltered data. Also, note that there is no phase lag in these filtered data because of the dual forward and reverse filtering processes.

3.4.4.3 Choice of Cutoff Frequency—Residual Analysis. There are several ways to choose the best cutoff frequency. The first is to carry out a harmonic analysis as depicted in Figure 3.16. By analyzing the power in each of the components, a decision can be made as to how much power to accept and how much to reject. However, such a decision assumes that the filter is ideal and has an infinitely sharp cutoff. A better method is to do a residual analysis of the difference between filtered and unfiltered signals over a wide range of cutoff frequencies (Wells and Winter, 1980). In this way, the characteristics of the filter in the transition region are reflected in the decision process. Figure 3.20 shows a theoretical plot of residual versus frequency. The residual at any cutoff frequency is calculated as follows [see Equation (3.9)] for a signal of N sample points in time:

$$R(f_c) = \sqrt{\frac{1}{N}\sum_{i=1}^{N}(X_i - \hat{X}_i)^2} \tag{3.9}$$

where f_c = is the cutoff frequency of the fourth-order dual-pass filter.
X_i = is raw data at ith sample.
$\hat{X}_i$ = is filtered data at the ith sample using a fourth-order zero-lag filter.

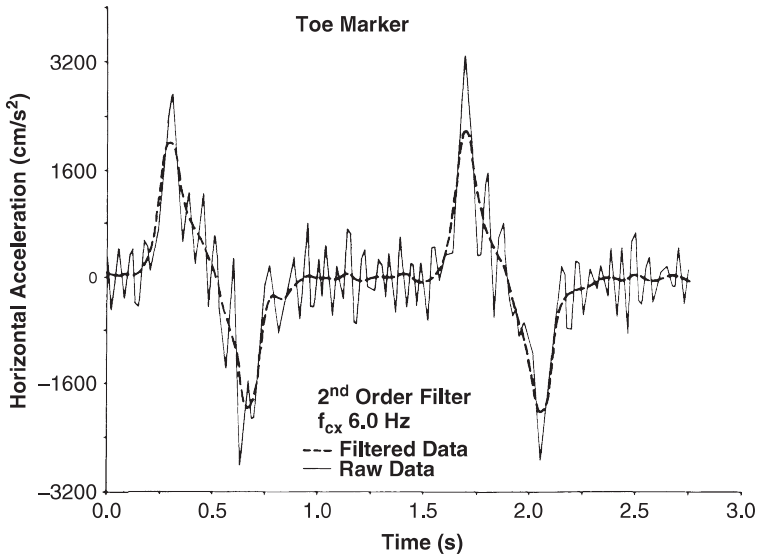

Figure 3.19 Horizontal acceleration of the toe marker during normal walking as calculated from displacement data from television. The solid line is the acceleration based on the unprocessed "raw" data; the dotted line is that calculated after the data has been filtered with a fourth-order zero-lag low-pass digital filter. (Reproduced by permission from the *Journal of Biomechanics.*)

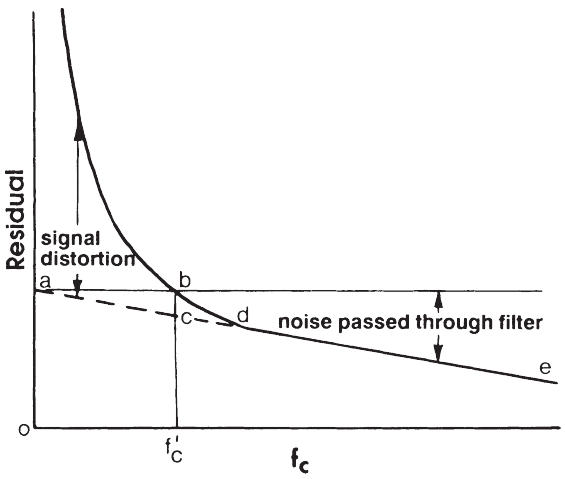

Figure 3.20 Plot of the residual between a filtered and an unfiltered signal as a function of the filter cutoff frequency. See text for the interpretation as to where to set the cutoff frequency of the filter.

If our data contained no signal, just random noise, the residual plot would be a straight line decreasing from an intercept at 0 Hz to an intercept on the abscissa at the Nyquist frequency (0.5 f_s). The line *de* represents our best estimate of that noise residual. The intercept *a* on the ordinate (at 0 Hz) is nothing more than the rms value of the noise, because $\hat{X}_i$ for a 0-Hz filter is nothing more than the mean of the noise over the N samples. When the data consist of true signal plus noise, the residual will be seen to rise above the straight (dashed) line as the cutoff frequency is reduced. This rise above the dashed line represents the signal distortion that is taking place as the cutoff is reduced more and more.

The final decision is where f_c should be chosen. The compromise is always a balance between the signal distortion and the amount of noise allowed through. If we decide that both should be equal, then we simply project a line horizontally from *a* to intersect the residual line at *b*. The frequency chosen is f_c^1, and at this frequency the signal distortion is represented by *bc*. This is also an estimate of the noise that is passed through the filter. Figure 3.21 is a plot of the residual of four markers from one stride of gait data, and both vertical and horizontal coordinates were analyzed (Wells and Winter, 1980). As can be seen, the straight regression line that represents the noise is essentially the same for both coordinates on all markers. This tells

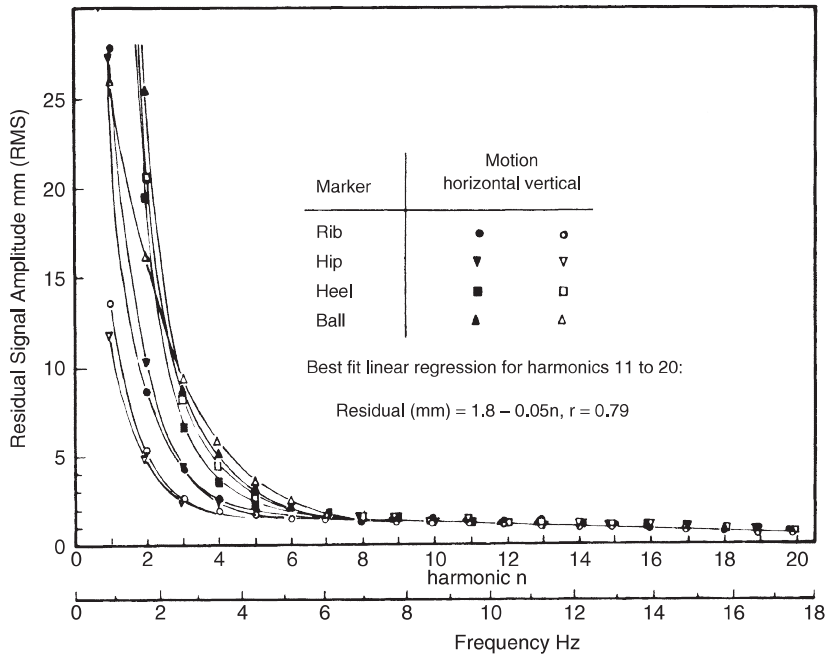

Figure 3.21 Plot of the residual of four markers from a walking trial; both vertical and horizontal displacement data. Data were digitized from movie film with the camera 5 m from the subject.

us that the noise content, mainly introduced by the human digitizing process, is the same for all markers. This regression line has an intercept of 1.8 mm, which indicates that the rms of the noise is 1.8 mm. In this case, the cine camera was 5 m from the subject and the image was 2 m high by 3 m wide. Thus, the rms noise is less than one part in 1000.

Also, we see distinct differences in the frequency content of different markers. The residual shows the more rapidly moving markers on the heel and ball to have power up to about 6 Hz, while the vertical displacements of the rib and hip markers were limited to about 3 Hz. Thus, through this selection technique, we could have different cutoff frequencies specified for each marker displacement.

3.4.4.4 Optimal Cutoff Frequency. The residual analysis technique described in the previous section suggested the choice of a frequency where the signal distortion was equal to the residual noise. This optimal applies to displacement data only. However, this may not be the optimum frequency for all amplitudes of signal and noise, all sampling frequencies, and all levels of differentiation: velocities versus accelerations. Giakas and Baltzopoulos (1997) showed that the optimal cutoff frequencies depended on noise level and whether displacements, velocities, or accelerations were being considered. Unfortunately, their reference displacement signal was reconstituted from a harmonic analysis, and in Section 2.2.4.5 this technique was shown to have major problems because of lack of stationarity of each harmonics amplitude and phase. Yu et al. (1999) carried out a detailed analysis to estimate the optimum cutoff frequency for higher-order derivatives, especially accelerations. They found the optimum cutoff frequencies to be somewhat higher than those estimated for the displacement residual analysis. This is not suprising when we consider that the acceleration increases as the square of the frequency (Section 3.4.3); thus, the higher-frequency noise in the acceleration waveform will increase far more rapidly than the signal itself. Also, when the sampling frequency, f_s, increases, the sampling period, $\Delta t = 1/f_s$, decreases, and thus the noise as calculated by finite differences increases [see Equations (3.17) and (3.18c)]. Thus, Yu et al. (1999) estimated that the optimum cutoff frequency was not only a function of the residual between the filtered and unfiltered data but also a function of f_s. Their estimated optimal cutoff frequency, $f_{c.2}$, was:

$$f_{c,2} = 0.06\, f_s - 0.000022\, f_s^2 + 5.95/\boldsymbol{\varepsilon} \tag{3.10}$$

where f_s is the sampling frequency and $\boldsymbol{\varepsilon}$ is the relative mean residual between X_i and $\hat{X}_i$ [terms defined in Equation (3.9)]. These authors present example acceleration curves (see Figure 3.4 in Yu et al.,1999) that shows a reasonable match between the accelerometer data and the filtered film data, except that the lag of the filtered data suggests that a second-order low-pass filter was used rather than the desired fourth-order zero-lag filter.

3.4.5 Comparison of Some Smoothing Techniques

It is valuable to see the effect of several different curve-fitting techniques on the same set of noisy data. The following summary of a validation experiment, which was conducted to compare (Pezzack et al., 1977) three commonly used techniques, illustrates the wide differences in the calculated accelerations.

Data obtained from the horizontal movement of a lever arm about a vertical axis were recorded three different ways. A goniometer on the axis recorded angular position, an accelerometer mounted at the end of the arm gave tangential acceleration and thus angular acceleration, and cinefilm data gave image information that could be compared with the angular and acceleration records. The comparisons are given in Figure 3.22. Figure 3.22*a* compares the angular position of the lever arm as it was manually moved from rest through about 130° and back to the original position. The goniometer signal and the lever angle as analyzed from the film data are plotted and compare closely. The only difference is that the goniometer record is somewhat noisy compared with the film data.

Figure 3.22*b* compares the directly recorded angular acceleration, which can be calculated by dividing the tangential acceleration by the radius of the accelerometer from the center of rotation, with the angular acceleration as calculated via the second derivative of the digitally filtered coordinate data (Winter et al., 1974). The two curves match extremely well, and the finite-difference acceleration exhibits less noise than the directly recorded acceleration. Figure 3.22*c* compares the directly recorded acceleration with the calculated angular acceleration, using a polynomial fit on the raw angular data. A ninth-order polynomial was fitted to the angular displacement curve to yield the following fit:

$$\begin{aligned}\boldsymbol{\theta}(t) = {} & 0.064 + 2.0t - 35t^2 + 210t^3 - 430t^4 + 400t^5 \\ & - 170t^6 + 25t^7 + 2.2t^8 - 0.41t^9 \text{ rad}\end{aligned} \tag{3.11}$$

Note that $\boldsymbol{\theta}$ is in radians and t in seconds. To get the curve for angular acceleration, all we need to do is take the second time derivative to yield:

$$\begin{aligned}\boldsymbol{\alpha}(t) = {} & -70 + 1260t - 5160t^2 + 8000t^3 - 5100t^4 \\ & + 1050t^5 + 123t^6 - 29.5t^7 \text{ rad/s}^2\end{aligned} \tag{3.12}$$

This acceleration curve, compared with the accelerometer signal, shows considerable discrepancy, enough to cast doubt on the value of the polynomial fit technique. The polynomial is fitted to the displacement data in order to get an analytic curve, which can be differentiated to yield another smooth curve. Unfortunately, it appears that a considerably higher-order polynomial would be required to achieve even a crude fit, and the computer time might become too prohibitive.

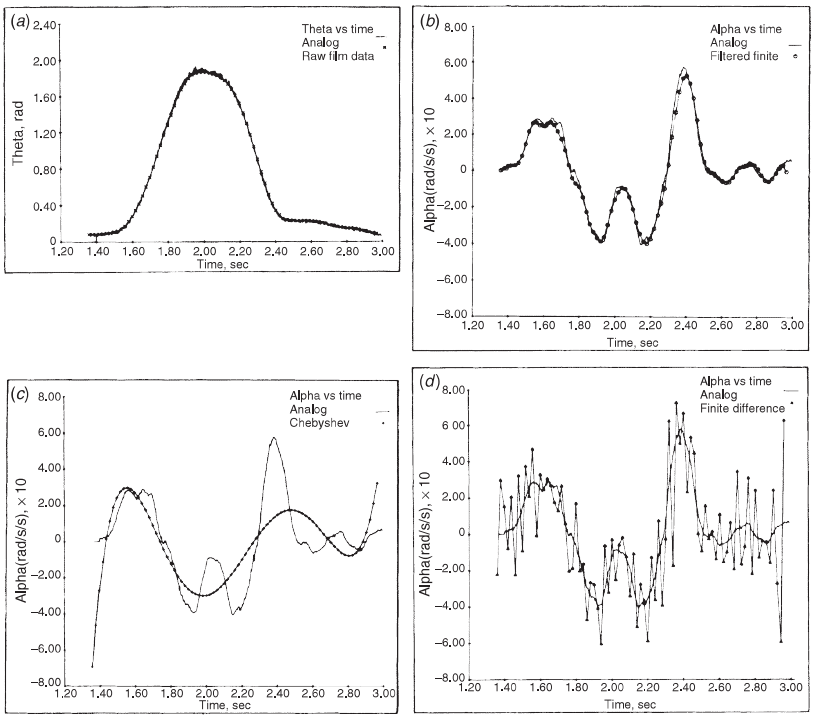

Figure 3.22 Comparison of several techniques used to determine the acceleration of a movement based on film displacement data. (a) Displacement angle of a simple extension/flexion as plotted from film and goniometer data. (b) Acceleration of the movement in (a) as measured by an accelerometer and as calculated from film coordinates after digital filtering. (c) Acceleration as determined from a ninth-order polynomial fit of the displacement data compared with the directly recorded acceleration. (d) Acceleration as determined by finite-difference technique of the raw coordinate data compared with the accelerometer curve. (Reproduced by permission from the Journal of Biomechanics.)

Finally, in Figure 3.22*d*, you can see the accelerometer signal plotted against angular acceleration as calculated by second-order finite-difference techniques using raw coordinate data. The plot speaks for itself—the accelerations are too noisy to mean anything.

3.5 CALCULATION OF OTHER KINEMATIC VARIABLES

3.5.1 Limb-Segment Angles

Given the coordinate data from anatomical markers at either end of a limb segment, it is an easy step to calculate the absolute angle of that segment in space. It is not necessary that the two markers be at the extreme ends of the limb segment, as long as they are in line with the long-bone axis. Figure 3.23

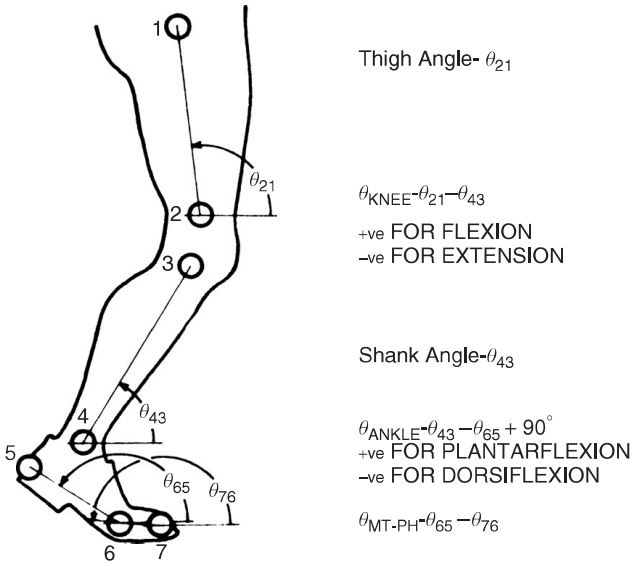

Figure 3.23 Marker location and limb and joint angles using an established convention. Limb angles in the spatial reference system are determined using counterclockwise from the horizontal as positive. Thus, angular velocities and accelerations are also positive in the counterclockwise direction in the plane of movement; this is essential for consistent convention use in subsequent kinetic analyses. Conventions for joint angles (which are relative) are subject to wide variation among researchers; thus, the convention used must be clarified.

shows the outline of a leg with seven anatomical markers in a four-segment three-joint system. Markers 1 and 2 define the thigh in the sagittal plane. Note that, by convention, all angles are measured in a counterclockwise direction, starting with the horizontal equal to 0°. Thus, $\boldsymbol{\theta}_{43}$ is the angle of the leg in space and can be calculated from:

$$\boldsymbol{\theta}_{43} = \arctan\frac{y_3 - y_4}{x_3 - x_4} \tag{3.13}$$

or, in more general notation,

$$\boldsymbol{\theta}_{ij} = \arctan\frac{y_j - y_i}{x_j - x_i} \tag{3.14}$$

As has already been noted, these segment angles are absolute in the defined spatial reference system. It is, therefore, quite easy to calculate the joint angles from the angles of the two adjacent segments.

3.5.2 Joint Angles

Each joint has a convention for describing its magnitude and polarity. For example, when the knee is fully extended, it is described as 0° flexion, and when the leg moves in a posterior direction relative to the thigh, the knee is said to be in flexion. In terms of the absolute angles described previously,

$$\text{knee angle} = \boldsymbol{\theta}_k = \boldsymbol{\theta}_{21} - \boldsymbol{\theta}_{43}$$

If $\boldsymbol{\theta}_{21} > \boldsymbol{\theta}_{43}$, the knee is flexed; if $\boldsymbol{\theta}_{21} < \boldsymbol{\theta}_{43}$, the knee is extended.

The convention for the ankle is slightly different in that 90° between the leg and the foot is boundary between plantarflexion and dorsiflexion. Therefore,

$$\text{ankle angle} = \boldsymbol{\theta}_a = \boldsymbol{\theta}_{43} - \boldsymbol{\theta}_{65} + 90^\circ$$

If $\boldsymbol{\theta}_a$ is positive, the foot is plantarflexed; if $\boldsymbol{\theta}_a$ is negative, the foot is dorsiflexed.

3.5.3 Velocities—Linear and Angular

As was seen in Section 3.4.3, there can be severe problems associated with the determination of velocity and acceleration information. For the reasons outlined, we will assume that the raw displacement data have been suitably smoothed by digital filtering and we have a set of smoothed coordinates and angles to operate upon. To calculate the velocity from displacement data, all that is needed is to take the finite difference. For example, to determine the velocity in the x direction, we calculate $\Delta x/\Delta t$, where $\Delta x = x_{i+1} - x_i$, and Δt is the time between adjacent samples x_{i+1} and x_i.

The velocity calculated this way does not represent the velocity at either of the sample times. Rather, it represents the velocity of a point in time halfway between the two samples. This can result in errors later on when we try to relate the velocity-derived information to displacement data, and both results do not occur at the same point in time. A way around this problem is to calculate the velocity and accelerations on the basis of $2\Delta t$ rather than Δt. Thus, the velocity at the ith sample is:

$$Vx_i = \frac{x_{i+1} - x_{i-1}}{2\Delta t}\text{m/s} \tag{3.15}$$

Note that the velocity is at a point halfway between the two samples, as depicted in Figure 3.24. The assumption is that the line joining x_{i-1} to x_{i+1} has the same slope as the line drawn tangent to the curve at x_i.

For angular velocities, the formula is the same except that we use angular data rather than displacement data in Equation (3.14); the angular acceleration

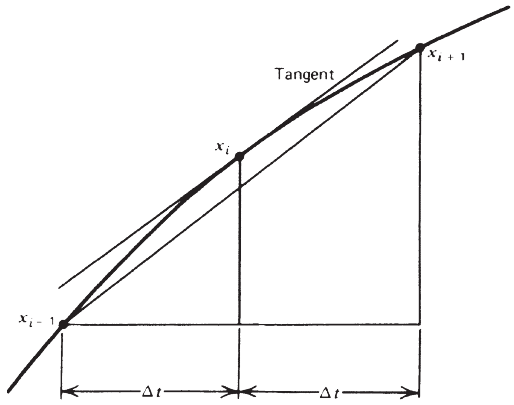

Figure 3.24 Finite-difference technique for calculating the slope of a curve at the ith sample point.

at the ith sample is:

$$\omega_i = \frac{\theta_{i+1} - \theta_{i-1}}{2\Delta t} \text{ rad/s} \tag{3.16}$$

3.5.4 Accelerations—Linear and Angular

Similarly, the acceleration is:

$$Ax_i = \frac{Vx_{i+1} - Vx_{i-1}}{2\Delta t} \text{ m/s}^2 \tag{3.17}$$

Note that Equation (3.16) requires displacement data from samples $i + 2$ and $i - 2$; thus, a total of five successive data points go into the acceleration. An alternative and slightly better calculation of acceleration uses only three successive data coordinates and utilizes the calculated velocities halfway between sample times:

$$Vx_{i+1/2} = \frac{x_{i+1} - x_i}{\Delta t} \text{ m/s} \tag{3.18a}$$

$$Vx_{i-1/2} = \frac{x_i - x_{i-1}}{\Delta t} \text{ m/s} \tag{3.18b}$$

Substituting these "halfway" velocities into Equation (3.17) we get:

$$Ax_i = \frac{x_{i+1} - 2x_i + x_{i-1}}{\Delta t^2} \text{ m/s}^2 \tag{3.18c}$$

For angular accelerations merely replace displacement data with angular data in Equations (3.17) or (3.18).

3.6 PROBLEMS BASED ON KINEMATIC DATA

1. Tables A.1 and A.2 in Appendix A, plot the vertical displacement of the raw and filtered data (in centimeters) for the greater trochanter (hip) marker for frames 1 to 30. Use a vertical scale as large as possible so as to identify the noise content of the raw data. In a few lines, describe the results of the smoothing by the digital filter.

2. Using filtered coordinate data (see Table A.2), plot the vertical displacement of the heel marker from TOR (frame 1) to the next TOR (frame 70).

(a) Estimate the instant of heel-off during midstance. (*Hint:* Consider the elastic compression and release of the shoe material when arriving at your answer.)

(b) Determine the maximum height of the heel above ground level during swing. When does this occur during the swing phase? (*Hint:* Consider the lowest displacement of the heel marker during stance as an indication of ground level.)

(c) Describe the vertical heel trajectory during the latter half of swing (frames 14–27), especially the four frames immediately prior to HRC.

(d) Calculate the vertical heel velocity at HRC.

(e) Calculate from the horizontal displacement data the horizontal heel velocity at HCR.

(f) From the horizontal coordinate data of the heel during the first foot flat period (frames 35–40) and the second foot flat period (frames 102–106), estimate the stride length.

(g) If one stride period is 69 frames, estimate the forward velocity of this subject.

3. Plot the trajectory of the trunk marker (rib cage) over one stride (frames 28–97).

(a) Is the shape of this trajectory what you would expect in walking?

(b) Is there any evidence of conservation of mechanical energy over the stride period? (That is, is potential energy being converted to kinetic energy and vice versa?)

4. Determine the vertical displacement of the toe marker when it reaches its lowest point in late stance and compare that with the lowest point during swing, and thereby determine how much toe clearance took place. *Answer:* $y_{\text{toe}}(\text{fr.13}) = 0.0485$ m, $y_{\text{toe}}(\text{fr.66}) = 0.0333$ m, clearance $= 0.0152\,\text{m} = 1.52$ cm.

5. From the filtered coordinate data (see Table A.2), calculate the following and check your answer with that listed in the appropriate listings (see Tables A.2, A.3, and A.4).

(a) The velocity of the knee in the X direction for frame 10.

(b) The acceleration of the knee in the X direction for frame 10.

(c) The angle of the thigh and leg in the spatial reference system for frame 30.

(d) From (c) calculate the knee angle for frame 30.

(e) The absolute angular velocity of the leg for frame 30 (use angular data, Table A.3).

(f) Using the tabulated vertical velocities of the toe, calculate its vertical acceleration for frames 25 and 33.

6. From the filtered coordinate data in Table A.2, calculate the following and check your answer from the results tabulated in Table A.3.

(a) The center of mass of the foot segment for frame 80.

(b) The velocity of the center of mass of the leg for frame 70. Give the answer in both coordinate and polar form.

3.7 REFERENCES

Dinn, D. F., D. A. Winter, and B. G. Trenholm. "CINTEL-Computer Interface for Television," *IEEE Trans. Computers* **C-19**: 1091–1095, 1970.

Eberhart, H. D. and V. T. Inman. "An Evaluation of Experimental Procedures Used in a Fundamental Study of Human Locomotion," *Ann. NY Acad. Sci.* **5**: 1213–1228, 1951.

Ferrigno, G. and A. Pedotti. "ELITE: A Digital Dedicated Hardware System for Movement Analysis via Real-Time TV Signal Processing," *IEEE Trans. Biomed. Eng.* **32**: 943–950, 1985.

Finley, F. R. and P. V. Karpovich. "Electrogoniometric Analysis of Normal and Pathological Gaits," *Res. Quart.* **35**: 379–384, 1964.

Furnée, E. H. 1967. *See* Woltring, 1987.

Gage, W. G., D. A. Winter, J. S. Frank, and A. L. Adkin. "Kinematic and Kinetic Validation of Inverted Pendulum Model in Quiet Standing," *Gait and Posture*, **19**: 124–132, 2004.

Giakas, G. and V. Baltzopoulos. "Optimal Digital Filtering Requires a Different Cut-off Frequency Strategy for Determination of the Higher Frequency Derivatives," *J. Biomech.* **30**: 851–855, 1997.

Jarett, M. O., B. J. Andrews, and J. P. Paul. "A Television/Computer System for the Analysis of Human Locomotion," *Proc. IERE Conf. on Applications of Electronics in Medicine*, Southhampton, England, 1976.

Macleod, A., J. R. W. Morris, and M. Lyster. "Close-Range Photogrammetry Meets Machine Vision," *SPIE Vol. 1395*, A. Gruen and E. Baltsavias, Eds. 1990, pp. 12–17. Bellingham, WA.

Moore, A., R. Wells, and D. Ranney. "Quantifying Exposure in Occupational Manual Tasks with Cumulative Trauma Disorder Potential," *Ergonomics* **34**: 1433–1453, 1991.

Morris, J. R.W. "Accelerometry-A Technique for the Measurement of Human Body Movements," *J. Biomech.* **6**: 729–736, 1973.

Pezzack, J. C., R. W. Norman, and D. A. Winter, "An Assessment of Derivative Determining Techniques Used for Motion Analysis," *J. Biomech.* **10**: 377–382, 1977.

Trenholm, B. G., D. A. Winter, D. Mymin, and E. L. Lansdown, "Computer Determination of Left Ventricular Volume Using Videodensitometry," *Med. & Biol. Eng.* **10**: 163–173, 1972.

Wells, R. P., D. A. Winter, "Assessment of Signal and Noise in the Kinematics of Normal, Pathological and Sporting Gaits," *Proc. 1st Conf. Cdn. Soc. Biomech., Locomotion I,* London, Ont., 1980.

Winter, D. A., S. A. Malcolm, and B. G. Trenholm, "System for Real-Time Conversion of Video Images of Physiological Events," *Proc. 21st Conf. Engineering in Medicine & Biol*., Houston, Texas, 1968.

Winter, D. A., R. K. Greenlaw, and D. A. Hobson. "Television-Computer Analysis of Kinematics of Human Gait," *Computers Biomed. Res.* **5**: 498–504, 1972.

Winter, D. A., H. G. Sidwall, and D. A. Hobson. "Measurement and Reduction of Noise in Kinematics of Locomotion," *J. Biomech.* **7**: 157–159, 1974.

Winter, D. A., A. E. Patla, M. G. Ishac, and W. H. Gage. "Motor Mechanisms of Balance During Quiet Standing," *J: Electromyogr. Kinesiol.* **13**: 49–56, 2003.

Woltring, H. J. "Data Acquisition and Processing Systems in Functional Movement Analysis." *Minerva Orthop. Traumatol.* **38**: 703–716, 1987.

Yu, B., D. Gabriel, L. Noble, and K. An. "Estimate of Optimum Cutoff Frequency for the Butterworth Low-Pass Digital Filter," *J. Appl. Biomech.* **15**: 318–329, 1999.